RSC Advances

PAPER

View Article Online
View Journal | View Issue

Check for updates

Cite this: *RSC Adv.*, 2023, **13**, 16712

Esterification of fluorinated aromatic carboxylic acids with methanol by using UiO-66-NH_2 as a heterogeneous catalyst and process optimization by the Taguchi method†

Anuj Kumar, Satish Kumar Singh and Chhaya Sharma *

Fluorobenzoic acids (FBAs) are used as chemical tracers in enhanced oil recovery and reduction in their limit of detection is a crucial issue. GC-MS is a versatile tool to detect and quantify FBAs at very low limits of concentration, but they require esterification prior to analysis by GC-MS. The present article presents a study of the catalytic methyl esterification of fluorinated aromatic carboxylic acids (FBAs) using methanol as methyl source and UiO-66-NH_2 as a heterogeneous catalyst. The reaction time was reduced to 10 hours which is a 58% reduction in time over the traditional BF_3·MeOH complex as derivatizing agent. The yield of the esterification reaction was evaluated with respect to the BF_3–MeOH complex and determined by GC-EI-MS. The catalytic procedure was optimized by the Taguchi model with a 99.99% fit. Good catalytic performance was observed for 23 different isomers of fluorinated aromatic acids showing a relative conversion yield of up to 169.86%, which reduced the detection limit of FBAs up to 2.60 ng mL^{-1}.

Received 27th March 2023
Accepted 20th May 2023

DOI: 10.1039/d3ra02005c

rsc.li/rsc-advances

Open Access Article. Published on 02 June 2023. Downloaded on 5/17/2026 5:32:05 AM.
This article is licensed under a Creative Commons Attribution-NonCommercial 3.0 Unported Licence.

1. Introduction

The need to detect groundwater flow, leachates from waste disposal sites, hydrogeological studies, and the testing of inter-well tracers for enhanced oil recovery (EOR) are the two main factors that have led to the scientific exploration of various chemical compounds to be used as a tracer in recent years. Fluorobenzoic acids (FBAs) are chemical compounds used as chemical tracers in EOR. For maximum oil recovery, the reservoir fluid is mobilized by the flooding at the injector well towards the producer well. The producer well is sampled periodically to analyze the concentration of tracers. The analysis of the FBAs is usually done by various analytical tools like GC-MS, LC-MS, and IC-MS, *etc.*, as Kumar *et al.*[1] described in their review article. Different analytical tools are based on different principles and offer different detection limits. GC-based methods are very suitable methods to obtain a lower limit of detection (LOD) after the derivatization step before the analysis. The process for the esterification of FBAs was described by Muller *et al.*[2] and Galdiga *et al.*[3] The former study used BF_3·MeOH as a derivatizing agent, which requires 24 hours for the completion of the reaction. The latter study described diazomethane for the methyl esterification of FBAs, but the use of diazomethane is now discontinued due to its high toxicity. Some other GC-based methods are also available, but they require chemical ionization (CI) source along with the reagent gas like methane.[4] Also, the derivatizing agent, like pentafluorobenzyl bromide used in CI,[4] is a lachrymator and may create many side products as ghost peaks in the chromatogram.[5] The solid heterogeneous catalyst can overcome this disadvantage as they can be easily separated from the reaction mixture and can be reused for repeated experiments, as compared by Chopade *et al.*[6] Many authors reported using heterogeneous catalysts in esterification/transesterification reactions.[6–11] Several heterogeneous catalysts such as zeolites, silicates, and metallic salts have been studied for esterification reactions, but MOF provides high selectivity as they are organic/inorganic hybrids and show both organic and inorganic properties. The acidic and basic sites of UiO-66-NH_2 involved in the esterification reactions are well explained by Caratelli *et al.*[12] while performing the Fisher esterification of carboxylic acids.

Further, MOFs are crystalline porous hybrid materials and possess high surface area, porosity, and chemical tunability due to their hollow structure. In MOFs, catalytically active centers can be introduced during or after synthesis. The free coordination sites serve as catalytically active Lewis-acid center functions. Additionally, the organic or inorganic portion of the framework can be functionalized, allowing additional catalytic components to be introduced into the MOF pores. UiO-66-NH_2 is formed by $Zr_6O_4(OH)_4$ type metallic clusters containing 6 Zr atoms linked with μ_3-O and μ_3-OH groups of the organic linker,

Department of Paper Technology, Indian Institute of Technology Roorkee, Saharanpur Campus, Saharanpur, Uttar Pradesh, 247001, India. E-mail: chhaya.sharma@pt.iitr.ac.in

† Electronic supplementary information (ESI) available. See DOI: https://doi.org/10.1039/d3ra02005c

© 2023 The Author(s). Published by the Royal Society of Chemistry

Open Access Article. Published on 02 June 2023. Downloaded on 5/17/2026 5:32:05 AM. This article is licensed under a Creative Commons Attribution-NonCommercial 3.0 Unported Licence.

i.e., BDC-NH_2. It also possesses excellent chemical stability due to metallic clusters' high degree of coordination. MOF catalyst has been previously reported in the esterification of long-chain fatty acid[13] and biodiesel production[8] but not reported for aromatic acids especially substituted with the strong electron-withdrawing atom like fluorine. The special reason for selecting the MOF with amino functionality is its higher catalytic activity for carboxylic acids than pristine UiO-66. The reason is the direct participation of the amino groups in the activation of the reaction substrate by assisting in the activation of the nucleophilic character of the alcohol and elimination of the water molecule.[13,14] All the FBAs contain F atom, which can participate in hydrogen bonding with the amino groups of UiO-66-NH_2 and assist in interaction between MOF and the FBAs that needs to be evaluated. It is another reason for selecting this particular functionality.

Manual one-factor-at-a-time (OFAT) optimization techniques are very slow and wasteful. Therefore, soft computational approaches, including techniques such as CCD (Central Composite Design), BBD (Box–Behnken Design), Taguchi OA (Orthogonal Array), and PBD (Plackett–Burman Design), are being used for process optimization. However, Taguchi OA is the best approach if you know the range and level of each tunable parameter that your process requires. It has already been reported as an optimization technique in many catalytic reactions.[15–25] This is because it mathematically eliminates many unnecessary parameter combinations and proposes only a certain number of significant runs sufficient to predict the optimal response.[19]

In this study, UiO-66-NH_2 was synthesized by using optimum conditions as per available methods in the literature and characterized by different techniques like XRD, FESEM with EDAX, FTIR, and BET to confirm its successful preparation. Then the aim was to check its catalytic activity in terms of conversion yield, selectivity and optimize the whole process using by suitable model. The hypothesis behind this study was that the increased conversion yield of esterification may affect the LOD of FBAs which is a crucial problem in tracer tests.

The UiO-66-NH_2 type MOF is employed as a catalyst in the methyl esterification of FBAs and has not been reported for the FBAs methyl esterification in the literature. Since the carbon atom of the FBAs carboxylic group is more electrophilic due to the electron-withdrawing nature of fluorine atom, the reaction is more feasible to facilitate the nucleophilic–electrophilic interaction. The reaction was carried out for 23 different isomers of FBAs to evaluate the impact of the degree of fluorination on the reaction yield, which was calculated with respect to $BF_3 \cdot MeOH$. The optimization of the catalytic procedure was done by the Taguchi L25 approach, while the statistical analysis was done by the analysis of variance (ANOVA), from which the regression model was developed for evaluating the relevance of different parameters. The obtained methyl esters of FBAs were characterized by gas chromatography coupled with mass spectrometry. Reusability tests for the synthesized catalyst were also done, reducing the overall cost and providing very good results.

2. Experimental

2.1. Materials, reagents, and synthesis of UiO-66-NH_2

All the FBAs (purity >98%), $ZrCl_4$, and 2-BDC-NH_2 were purchased from Sigma-Aldrich, USA. All solvents, including acetonitrile, hexane, and methanol, were gradient grade (Merck), and ultra-pure water was produced from the Milli-Q water purification system (Millipore-Merck, USA). Dimethyl formamide (DMF) and dichloromethane (DCM) were of analytical grade, purchased from Rankem. Autoclave assembly was purchased from the local supplier. The abbreviation and other details for FBAs have been provided in Table S1.†

The synthesis of Zr-based MOF was done by using previously reported methods[26,27] with some minor modifications. In a synthesis of MOF, 7.6 g $ZrCl_4$ and 3.6 g BDC-NH_2 were mixed in 72 mL DMF and transferred to a Teflon bomb, put at 150 °C for 24 hours. After the completion of the reaction, the yellow solid was washed 3–4 times with DMF and methanol to remove the unreacted part. The solvent exchange reaction was carried out using DCM at ambient conditions. Finally, the yellow powder was dried at 100 °C for 8 hours and activated at the same conditions prior to use for catalysis.

2.2. Instrumental measurements

The XRD pattern was recorded using Rigaku Ultima IV, Japan, in the angle range (2θ) of 5–80° at the scan rate of 5 °C min^{-1} using Cu Kα radiation ($\lambda = 0.15405$ nm). The USA model, FTIR spectrum 2 of PerkinElmer, was utilized to execute the FT-IR scans with a wavenumber bracket of 4000–600 cm^{-1}. For every sample, 32 scans were performed with a resolution of 4 cm^{-1} using KBr pellets of the sample made under 10-ton hydraulic pressure. The morphological study of MOF was done using a field emission scanning electron microscope (FESEM) MIRA3 FESEM TESCAN, USA, and the elemental analysis was done using an energy dispersive X-ray detector (EDAX) installed with this unit. The pore size determination and surface area analysis of the synthesized MOF was done by a surface area analyzer (Autosorb IQ, USA) based on Brunauer–Emmett–Teller (BET) theory. The degassing of the MOF was done at 120 °C for 8 hours before the analysis.

GC-MS analysis was performed on Trace GC Ultra (Thermo Fisher Scientific, USA) equipped with a split-less injector coupled to a DSQ series single quadrupole mass spectrometer with an electron impact (EI) source. The separation of FBAMEs was done on a TR-05 capillary column (60 m × 0.25 mm ID × 0.25 μm film thickness, Thermo Fisher Scientific, USA). The GC-MS conditions for analyzing FBAMEs are as follows:

High-purity helium was used as a carrier gas with the inline gas purifier; splitless injection; injection temperature 200 °C; MS transfer line temperature 280 °C; column head pressure; 150 kPa. The oven program was: Initial temperature 60 °C (held for 2 min), changed to 150 °C at a rate of 5.5 °C min^{-1} (held for 6 min), then increased to 250 °C at a rate of 25 °C min^{-1} and held for 6 min. The total run time required for one injection was 25 min. The mass spectrometer was operated in the EI mode with the ion source temperature of 230 °C and electron energy

Open Access Article. Published on 02 June 2023. Downloaded on 5/17/2026 5:32:05 AM.
This article is licensed under a Creative Commons Attribution-NonCommercial 3.0 Unported Licence.

of 70 eV. As reported by Muller *et al.*, chromatograms were acquired at the SIM ions of FBAMEs.[2] The MS detector was tuned to get the optimized response of the calibration gas, typically multiple of e^7.

2.3. Catalytic process

The typical flow diagram of the esterification process is shown in Fig. 1. The stock solutions of FBA are prepared in methanol and sonicated for at least 10 min for proper mixing. This solution was diluted further in methanol to get the desired concentration of FBAs. 5 mL of this solution was transferred to the separate volumetric flask, and 25 mg of MOF was added to it. This mixture was transferred to the Teflon bomb and put at 150 °C temperature for 10 hours. After the reaction completion, the solution was cooled until it attained room temperature. Thereafter, 1.0 mL Milli-Q water followed by 1.5 mL hexane was added to this solution and vortexed for 10 min to transfer the FBA methyl esters (FBAMEs) to the hexane layer. The hexane layer was collected carefully, and 1.0 μL of this solution was injected into spilt-less GC-MS. The reaction yield was calculated with respect to the area obtained for FBAMEs using $BF_3 \cdot MeOH$ as a methylating agent, using the below formula:

2.4. Design of experiments by Taguchi

The design of experiments was done by the Taguchi method. This method paves the way for the collation of data to determine factors that most influence the quality of the product with the minimal number of experiments to reduce precious time and resources. This method is very effective with the nominal number of parameters (3–50), with few significant interactions between them and a few contributing parameters. The least possible number of experiments N is decided from the number of levels L and the number of design and chosen control parameters P using the relation $N = (L \times P)$ in this particular study.

2.4.1. Selection of optimization parameters and their levels, orthogonal array of experiments. There are various parameters to be optimized for getting the maximum conversion yield of FBAMEs. Five parameters influencing the conversion yield, including sample volume, catalyst weight, reaction time, temperature, and hexane volume, were chosen at 5 levels ($L = 5$, $P = 5$, as shown in Table 1). The effect of the chosen parameters has been investigated by performing 25 experiments for each FBA. The experiments were repeated two times to confirm the repeatability of the results.

$$\%\ \text{relative conversion (RC)} = \frac{\text{area of FBAME by MOF methyl esterification}}{\text{area of FBAME by } BF_3 \cdot MeOH \text{ methyl esterification}} \times \frac{\text{conc. of FBAs used for } BF_3 \cdot MeOH \text{ methyl esterification}}{\text{conc. of FBAs used for MOF methyl esterification}} \times 100 \quad \text{(i)}$$

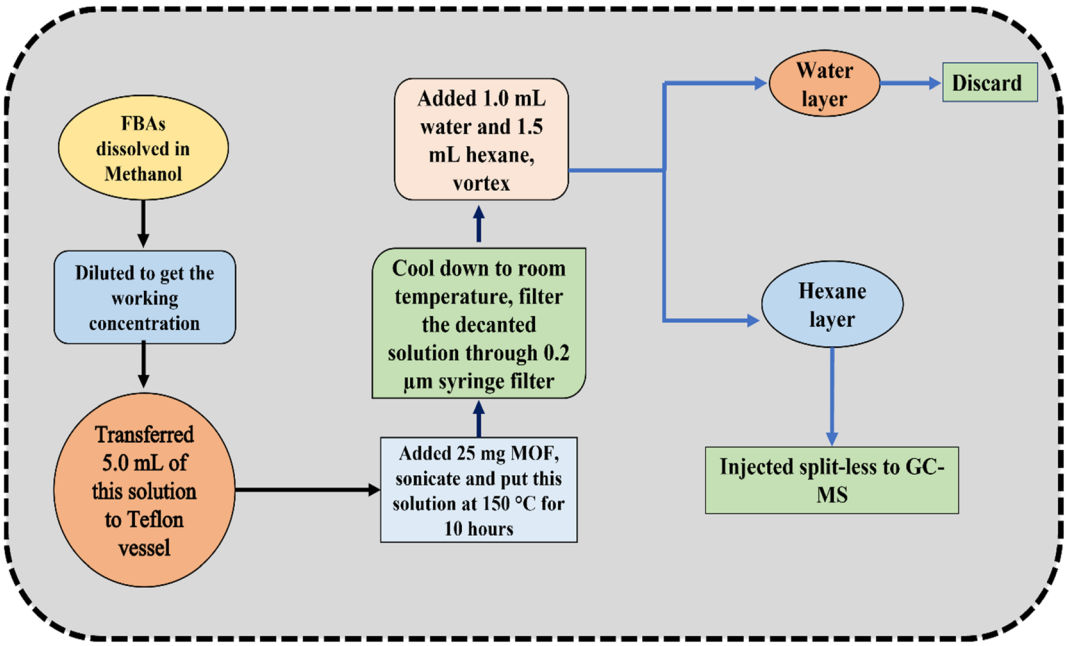

Fig. 1 Schematic describing the esterification procedure.

© 2023 The Author(s). Published by the Royal Society of Chemistry

Open Access Article. Published on 02 June 2023. Downloaded on 5/17/2026 5:32:05 AM.
This article is licensed under a Creative Commons Attribution-NonCommercial 3.0 Unported Licence.

Table 1 Chosen parameters and their levels

		Levels				
S. no.	Parameters	1	2	3	4	5
A	Sample volume (mL)	1	2	3	4	5
B	Weight of MOF (mg)	5	10	15	20	25
C	Time (h)	1	4	7	10	13
D	Temperature (°C)	64	100	120	150	170
E	Volume of hexane (mL)	1.5	2.0	3.0	4.0	5.0

The experiments were designed using an L25 array, and 25 experiments (Table 2) were needed to determine the optimum catalytic conditions.

2.4.2. Signal to noise ratio (SNR) and analysis of variance (ANOVA). Taguchi proposed using a loss function to calculate the deviation between experimental and target values for performance characteristics. The loss function values were further converted to signal-to-noise ratio (SNR). SNR is a log function of expected results that serves as a target for optimization problems and is used to calculate the amount of deviation of the quality function from its expected value. SNR has three types according to the purpose of the problem. One can use Large is Better (LB) for maximization problems, Smaller is Better (SB) for minimization problems, and Nominal is Best (NB) for regularization problems. The SNR (dB) for NTB, STB, and LTB models can be calculated as

$$\text{LB}: \text{SNR} = -10\log_{10}\frac{1}{n}\left(\sum_{i=1}^{n}\frac{1}{Y_i^2}\right) \quad \text{(ii)}$$

$$\text{NB}: \text{SNR} = -10\log_{10}\left(\frac{\overline{Y}^2}{s^2}\right) \quad \text{(iii)}$$

$$\text{SB}: \text{SNR} = -10\log_{10}\frac{1}{n}\left(\sum_{i=1}^{n}\frac{Y_i^2}{n}\right) \quad \text{(iv)}$$

where Y = mean value of the response, s^2 = variance, n = no. of experiments.

Since the objective of this study is to increase the yield of esterification, and this yield was calculated on the basis of GC-MS response. SNR ratio has been evaluated for the identification of optimal values of the selected parameters. In order to attain suitable conditions for maximum GC-MS response, LB SNR was chosen in the present study. However, the significant influence and contribution of the individual parameter cannot be estimated using this approach, so an ANOVA study was done for the recorded responses.

3. Results and discussions

3.1. Characterization of MOF

The Zr-based MOF was characterized by different analytical techniques. For crystallographic information, the XRD data (Fig. 2b-i) was acquired that corroborates with the previously reported literature.[28–30] The FESEM was done for the

Table 2 L25 orthogonal array for the design of experiments with 05 parameters at 05 levels

Experiment no.	Sample volume (mL)	Weight of catalyst (mg)	Reaction time (h)	Temperature (°C)	Volume of hexane (mL)
1	1	5	1	64	1.5
2	1	10	4	100	2.0
3	1	15	7	120	3.0
4	1	20	10	150	4.0
5	1	25	13	170	5.0
6	2	5	4	120	4.0
7	2	10	7	150	5.0
8	2	15	10	170	1.5
9	2	20	13	64	2.0
10	2	25	1	100	3.0
11	3	5	7	170	2.0
12	3	10	10	64	3.0
13	3	15	13	100	4.0
14	3	20	1	120	5.0
15	3	25	4	150	1.5
16	4	5	10	100	5.0
17	4	10	13	120	1.5
18	4	15	1	150	2.0
19	4	20	4	170	3.0
20	4	25	7	64	4.0
21	5	5	13	150	3.0
22	5	10	1	170	4.0
23	5	15	4	64	5.0
24	5	20	7	100	1.5
25	5	25	10	120	2.0

Open Access Article. Published on 02 June 2023. Downloaded on 5/17/2026 5:32:05 AM.
This article is licensed under a Creative Commons Attribution-NonCommercial 3.0 Unported Licence.

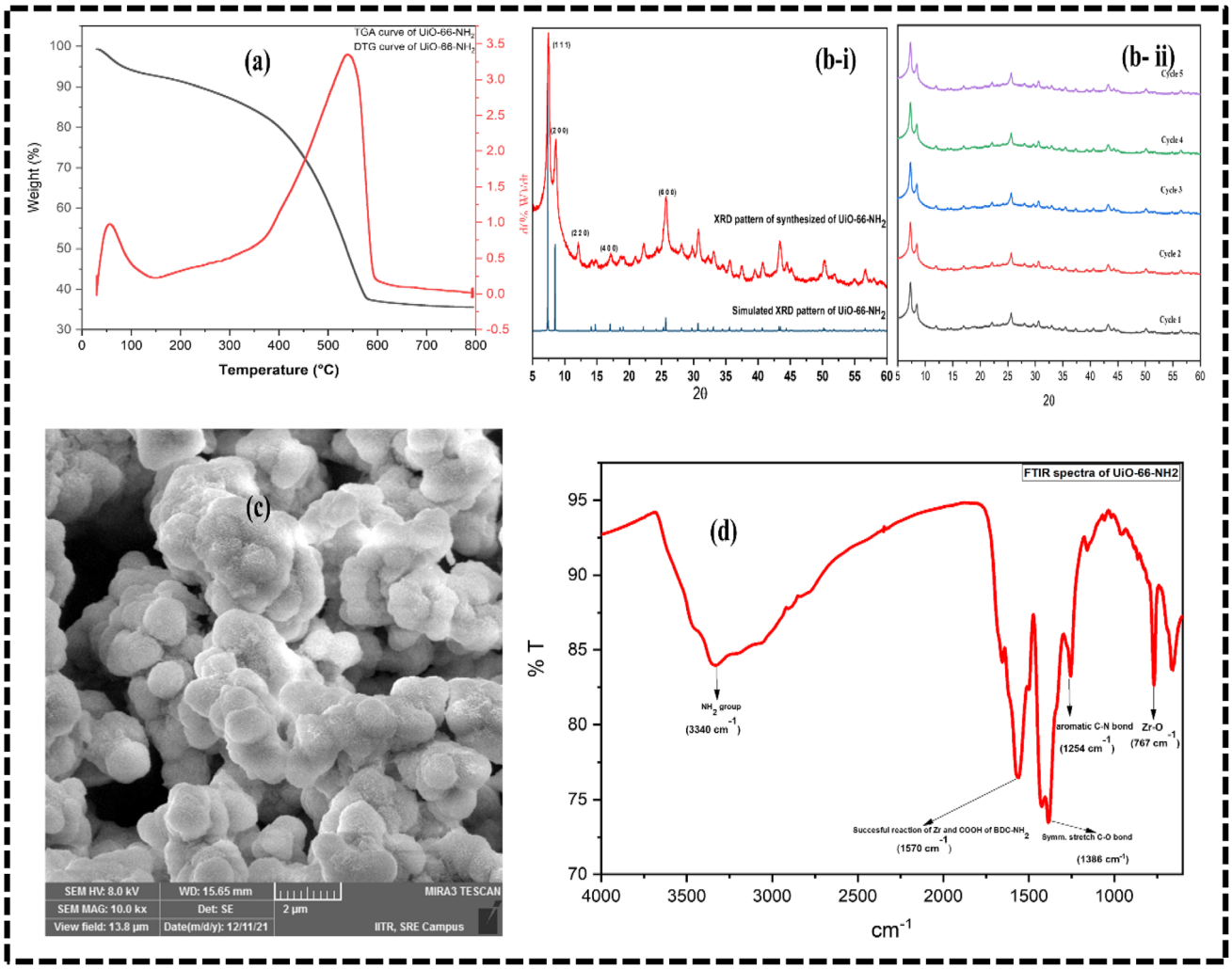

Fig. 2 (a) TGA/DTG curve (b-i & ii) XRD pattern and cyclic stability (c) FESEM image (d) FTIR spectra of synthesized UiO-66-NH_2.

morphology of the synthesized MOF that showed the spherical shape of the MOF particles (Fig. 2c). Furthermore, FTIR analysis was carried out using the KBr pellet method that showed the specific peak of the amino group at 3340 cm^{-1}, a specific peak at 1570 cm^{-1} corresponding to the successful reaction between Zr and the organic linker. The peaks at 767 cm^{-1}, 1254 cm^{-1}, and 1386 cm^{-1} were attributed to the Zr–O bond symmetric stretching, aromatic C–N bond, and symmetric stretching of the C–O bond, respectively (Fig. 2D).

The thermal degradation behavior of UiO-66-NH_2 was recorded using TGA (Fig. 2A), which showed the initial wt% loss of approximately 6% in the temperature range of 26 °C to 132 °C due to moisture in the sample. However, 5% and 50% weight loss were observed when the temperature was increased from 288 °C to 666 °C due to the decomposition of the organic linker and subsequent degradation of MOF, as reported in many literature.[29,30] The surface area and pore size distribution of the synthesized MOF were acquired by the BET surface area analyzer. As a result, the BET surface area and Langmuir surface area were found to be 301.992 $m^2\ g^{-1}$ and 374.389 $m^2\ g^{-1}$, respectively, with an average pore size of 9.671 Å.

3.2. Catalytic properties of UiO-66-NH_2

3.2.1. Esterification of 2,6 bis-FBA with MeOH. The methyl esterification of 2,6 bis-FBA could not be done using $BF_3 \cdot MeOH$ due to steric hindrance as reported by Muller *et al.*[2] This scenario was not experienced in this study, and successful conversion of 2,6 bis-FBA to its methyl ester with good conversion yield was obtained, so the potential analyte remained 23 in this study. It is another advantage that this catalytic process offered, but % relative conversion (RC) could not be calculated for this FBA as the conversion was not observed in the case of $BF_3 \cdot MeOH$.

3.2.2. Taguchi method for optimum conditions. The ANOVA statistical analysis was done to investigate the contribution of individual parameters on the relative conversion yield. The relative conversion yield was calculated on the basis of eqn (i) and shown in Table 4. Table 3 provides the *P*-value, *F*-value, and % contribution for each chosen parameter for different 23 isomers of FBAs. As it can be seen that the *P*-value for catalyst weight is very high in every individual data, so it is the least significant but important parameter for the study.

© 2023 The Author(s). Published by the Royal Society of Chemistry

Open Access Article. Published on 02 June 2023. Downloaded on 5/17/2026 5:32:05 AM.
This article is licensed under a Creative Commons Attribution-NonCommercial 3.0 Unported Licence.

Table 3 ANOVA results for different substituted FBAs[a]

Type of FBA	ANOVA data							
Mono FBA	Source	DF	Seq SS	Contribution	Adj SS	Adj MS	*F*-Value	*P*-Value
	SV	4	6.27×10^{12}	10.18%	6.27×10^{12}	1.56×10^{12}	3.09	0.15
	W	4	2.80×10^{12}	4.55%	2.80×10^{12}	7.00×10^{11}	1.38	0.38
	t	4	9.25×10^{12}	15.02%	9.25×10^{12}	2.31×10^{12}	4.56	0.08
	Temp	4	1.53×10^{13}	24.87%	1.53×10^{13}	3.83×10^{12}	7.55	0.03
	VH	4	2.59×10^{13}	42.09%	2.59×10^{13}	6.48×10^{12}	12.79	0.01
	Error	4	2.02×10^{12}	3.29%	2.02×10^{12}	5.07×10^{11}		
	Total	24	6.16×10^{13}	100.00%				
Di-FBA	Source	DF	Seq SS	Contribution	Adj SS	Adj MS	*F*-Value	*P*-Value
	SV	4	2.23×10^{11}	10.18%	2.23×10^{11}	5.59×10^{10}	3.09	0.15
	W	4	9.99×10^{10}	4.55%	9.99×10^{10}	2.49×10^{10}	1.38	0.38
	t	4	3.30×10^{11}	15.02%	3.30×10^{11}	8.25×10^{10}	4.56	0.08
	Temp	4	5.46×10^{11}	24.87%	5.46×10^{11}	1.36×10^{11}	7.55	0.03
	VH	4	9.24×10^{11}	42.09%	9.24×10^{11}	2.31×10^{11}	12.79	0.01
	Error	4	7.23×10^{10}	3.29%	7.23×10^{10}	1.80×10^{10}		
	Total	24	2.19×10^{12}	100.00%				
Tri-FBA	Source	DF	Seq SS	Contribution	Adj SS	Adj MS	*F*-Value	*P*-Value
	SV	4	5.93×10^{11}	9.62%	5.93×10^{11}	1.48×10^{11}	3.26	0.14
	W	4	2.41×10^{11}	3.91%	2.41×10^{11}	6.03×10^{10}	1.32	0.39
	t	4	9.03×10^{11}	14.63%	9.03×10^{11}	2.25×10^{11}	4.95	0.07
	Temp	4	1.53×10^{12}	24.82%	1.53×10^{12}	3.82×10^{11}	8.40	0.03
	VH	4	2.71×10^{12}	44.06%	2.71×10^{12}	6.79×10^{11}	14.91	0.01
	Error	4	1.82×10^{11}	2.95%	1.82×10^{11}	4.55×10^{10}		
	Total	24	6.17×10^{12}	100.00%				
Tetra-FBA	Source	DF	Seq SS	Contribution	Adj SS	Adj MS	*F*-Value	*P*-Value
	SV	4	2.98×10^{11}	10.18%	2.98×10^{11}	7.45×10^{10}	3.09	0.15
	W	4	1.33×10^{11}	4.55%	1.33×10^{11}	3.33×10^{10}	1.38	0.38
	t	4	4.39×10^{11}	15.02%	4.39×10^{11}	1.09×10^{11}	4.56	0.08
	Temp	4	7.28×10^{11}	24.87%	7.28×10^{11}	1.82×10^{11}	7.55	0.03
	VH	4	1.23×10^{12}	42.09%	1.23×10^{12}	3.08×10^{11}	12.79	0.01
	Error	4	9.64×10^{10}	3.29%	9.64×10^{10}	2.41×10^{10}		
	Total	24	2.92×10^{12}	100.00%				
Penta-FBA	Source	DF	Seq SS	Contribution	Adj SS	Adj MS	*F*-Value	*P*-Value
	SV	4	6.34×10^{10}	6.49%	6.34×10^{10}	1.58×10^{10}	1.65	0.32
	W	4	4.05×10^{10}	4.15%	4.05×10^{10}	1.01×10^{10}	1.05	0.48
	t	4	1.45×10^{11}	14.83%	1.45×10^{11}	3.62×10^{10}	3.77	0.11
	Temp	4	2.92×10^{11}	29.85%	2.92×10^{11}	7.30×10^{10}	7.59	0.03
	VH	4	3.98×10^{11}	40.75%	3.98×10^{11}	9.96×10^{10}	10.36	0.02
	Error	4	3.84×10^{10}	3.93%	3.84×10^{10}	9.62×10^{10}		
	Total	24	9.78×10^{11}	100.00%				
TFM-BA	Source	DF	Seq SS	Contribution	Adj SS	Adj MS	F-Value	*P*-Value
	SV	4	2.99×10^{11}	10.18%	2.99×10^{11}	7.48×10^{10}	3.09	0.15
	W	4	1.33×10^{11}	4.55%	1.33×10^{11}	3.34×10^{10}	1.38	0.38
	t	4	4.42×10^{11}	15.02%	4.42×10^{11}	1.10×10^{11}	4.56	0.08
	Temp	4	7.31×10^{11}	24.87%	7.31×10^{11}	1.82×10^{11}	7.55	0.03
	VH	4	1.23×10^{12}	42.09%	1.23×10^{12}	3.09×10^{11}	12.79	0.01
	Error	4	9.68×10^{10}	3.29%	9.68×10^{10}	2.42×10^{10}		
	Total	24	2.94×10^{12}	100.00%				
Bis-TFM-BA	Source	DF	Seq SS	Contribution	Adj SS	Adj MS	F-Value	*P*-Value
	SV	4	9.76×10^{10}	10.18%	9.76×10^{10}	2.44×10^{10}	3.09	0.15
	W	4	4.36×10^{10}	4.55%	4.36×10^{10}	1.09×10^{10}	1.38	0.38

Open Access Article. Published on 02 June 2023. Downloaded on 5/17/2026 5:32:05 AM. This article is licensed under a Creative Commons Attribution-NonCommercial 3.0 Unported Licence.

Table 3 (*Contd.*)

Bis-TFM-BA	Source	DF	Seq SS	Contribution	Adj SS	Adj MS	F-Value	*P*-Value
	t	4	1.44×10^{11}	15.02%	1.44×10^{11}	3.60×10^{10}	4.56	0.08
	Temp	4	2.38×10^{11}	24.87%	2.38×10^{11}	5.96×10^{10}	7.55	0.03
	VH	4	4.03×10^{11}	42.09%	4.03×10^{11}	1.00×10^{11}	12.79	0.01
	Error	4	3.15×10^{10}	3.29%	3.15×10^{10}	7.89×10^{10}		
	Total	24	9.59×10^{11}	100.00%				

[a] DF = degree of freedom, Seq SS = sequential sum of squares, Adj SS = adjusted sum of squares, Adj MS = adjusted mean squares.

Although the *P*-value for hexane volume is the least among all the parameters and % contribution for this parameter is up to 44%. Since the response of methyl esters is dependent upon the dilution or hexane volume, so it affects their response directly, but this parameter is not so important in terms of catalytic conversion. Excluding these two parameters, the temperature and time affect the reaction considerably, which is clear from Table 3 data stating their high % contribution. The similar contribution of SV, W, t, temp and VH was observed for mono-FBA, di-FBA, tri-FBA, tetra-FBA, penta-FBA, TFM-BA (trifluoromethyl substituted benzoic acid), and bis-TFM BA (bis trifluoromethyl substituted benzoic acid) so the ANOVA results fit to the results of individual substituted FBAs.

The regression model for each substituted FBAs was developed using 2nd order interaction among the parameters, and SV, VH, t and temp were included as the cross predictors in the particular model. Since the weight of MOF is the least significant parameter, it was excluded from the higher terms and the value of R^2 was found more than 99.99% as a result of this operation. The regression equation provided in Table S2† can be used as a model to calculate the response of FBAMEs and hence the % relative conversion yield.

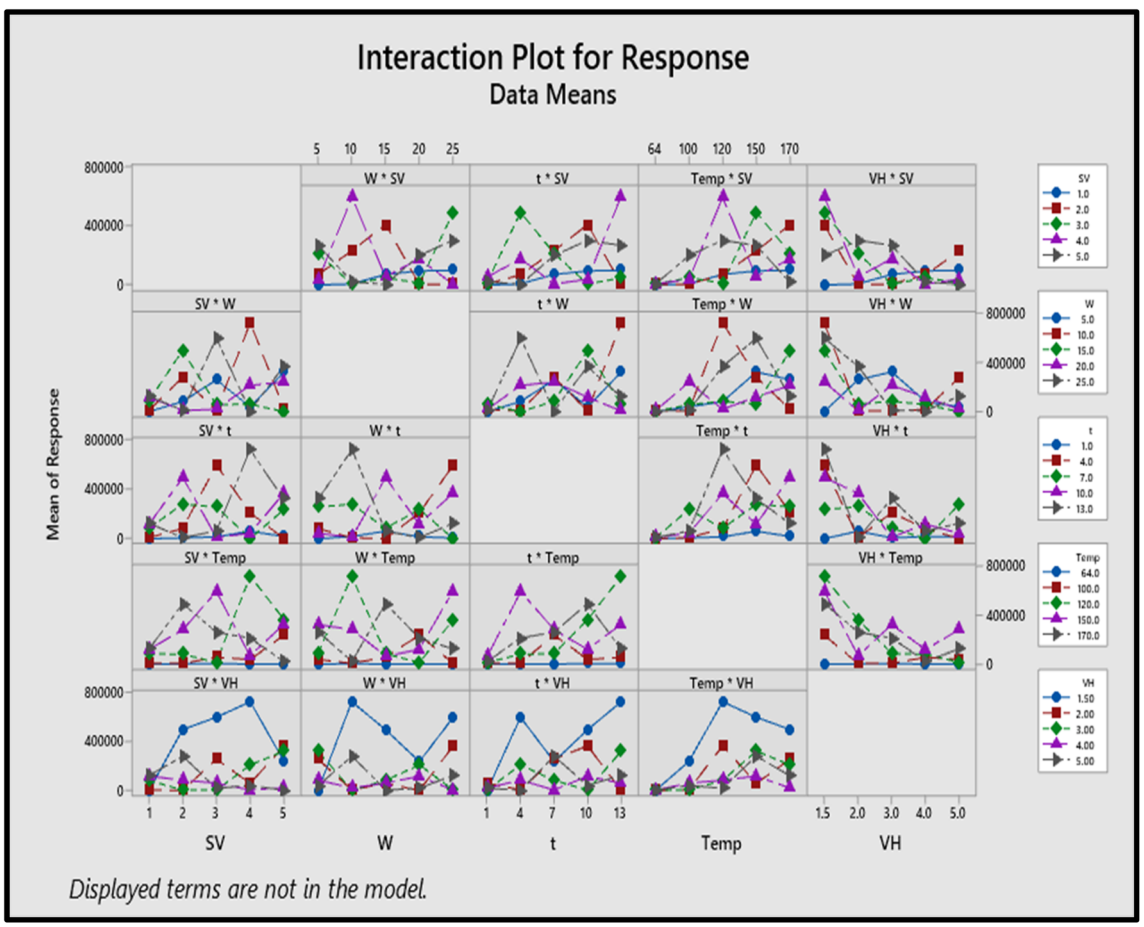

Fig. 3 Interaction plots between the chosen parameters.

© 2023 The Author(s). Published by the Royal Society of Chemistry

Open Access Article. Published on 02 June 2023. Downloaded on 5/17/2026 5:32:05 AM.
This article is licensed under a Creative Commons Attribution-NonCommercial 3.0 Unported Licence.

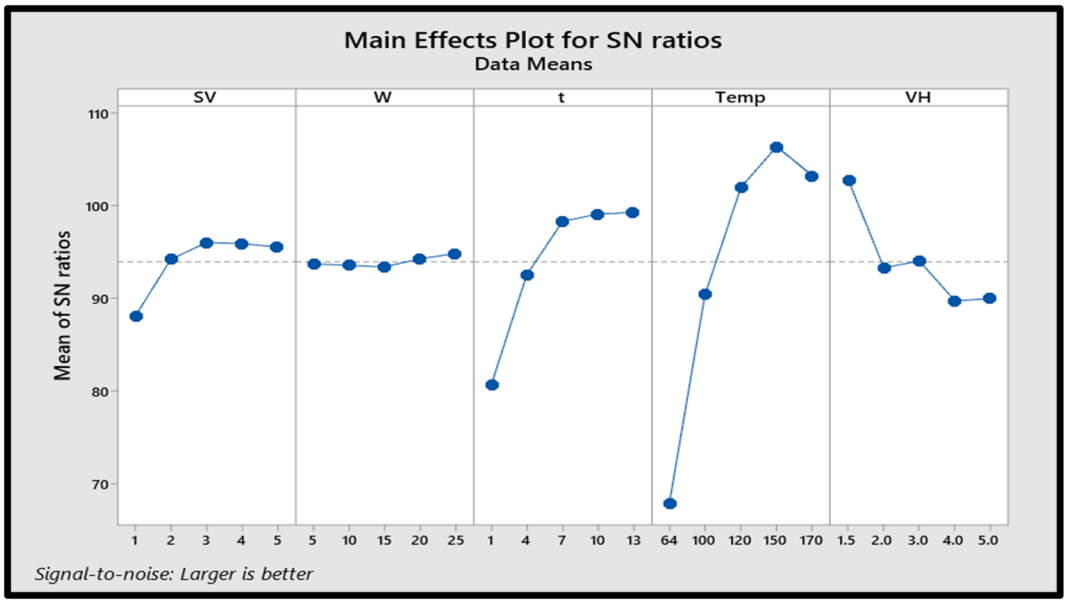

Fig. 4 SN ratio trend for different chosen parameters.

The interaction plot of individual parameters with the other parameters is shown in Fig. 3. Generally, the non-parallel line shows better interaction of parameters, and the parallel line shows the least interaction between the parameters. It is obvious from Fig. 3 that all the parameters are interconnected with each other except the volume of hexane (1.5 mL), as the highest response is obtained for this volume.

The optimum conversion from FBAs to their methyl esters was observed at 150 °C, a reaction time of 10 h, a sample volume of 5 mL, and 25 mg of MOF. When the temperature was increased from 150 °C to 170 °C, a gradual decrease in the conversion was seen, probably due to the degradation of methyl esters. Although, the increment in the conversion of FBAs to their methyl esters was seen when the temperature was increased from 64 °C to 120 °C and then to 150 °C. Since methanol is the only methyl esterification source in this reaction, its excess was required in the reaction; hence 5.0 mL of methanol containing FBAs was used as the optimized volume in the present study.

The amount of MOF was found to be the least influential parameter affecting the conversion of FBAs to their methylated product. Initially, a gradual decrease in the conversion was seen when the weight of MOF was increased from 5 mg to 15 mg, but a gradual increase in the conversion yield was noticed when the weight of MOF was further increased to 20 mg, and then the yield was found constant at 25 mg of MOF, so this amount was considered as an optimized condition for further study. The reaction time plays a crucial role in the completion of any chemical reaction. The present study was performed at 1 h, 3 h, 5 h, 7 h, and 10 h, but there was no considerable change found in the response of FBAME after 10 h. Since the volume of the extracting layer is always important in liquid–liquid extraction, the hexane volume ranging from 1.5 mL to 5.0 mL was added to the reaction. Although a higher volume of hexane may dilute the product concentration, it should be enough to extract the maximum concentration of methyl esters. 1.5 mL of hexane was found to be the suitable and optimum volume in the present study.

Fig. 4 represents the SNR trend for all substituted FBAs. The optimum conditions for the methyl esterification of FBAs were obtained on the basis of high SNR acquired using the Taguchi method. The procedure described in Section 1.2 was used to convert FBAs to their methyl esters. The optimum conditions were validated by triplicating the experiments at different concentration levels, as shown in Table 4. The resultant chromatograms are provided in Fig. S1.†

3.2.3. Kinetics of the reaction. The kinetic parameters of the reaction were calculated by considering the esterification reaction as a pseudo-first-order reaction. The reaction proceeds as follows:

$$\text{RF-COOH} + \text{CH}_3\text{OH} \xrightarrow{\text{UiO-66-NH}_2} \text{RF-COOCH}_3 + \text{H}_2\text{O}$$

The reaction rate expression for the above reaction can be written as:

$$r = \mathrm{d}C/\mathrm{d}t = -K[\text{RF-COOH}]\,[\text{CH}_3\text{OH}]$$

Since methanol is used in excess, the reaction can be considered zero order with respect to methanol; hence the final expression for the rate of reaction becomes;

$$r = \mathrm{d}C/\mathrm{d}t = -K[\text{RF-COOH}]$$

On separating the variables and integrating both sides,

$$\ln C_t = -K_t + \ln C_0 \qquad \text{(v)}$$

© 2023 The Author(s). Published by the Royal Society of Chemistry

Open Access Article. Published on 02 June 2023. Downloaded on 5/17/2026 5:32:05 AM. This article is licensed under a Creative Commons Attribution-NonCommercial 3.0 Unported Licence.

Table 4 % relative conversion of FBAs to FBAMEs with respect to BF_3·MeOH at two concentration levels, their LODs

S. no.	Component name	Concentration (ppb)	% RC (run-1)	% RC (run-2)	% RC (run-3)	LOD[a] (ng mL^{-1}) (n = 3)
1	2-FBA	511	146.43	143.51	148.46	3.08
		1022	134.73	136.47	134.43	
2	3-FBA	563	158.11	161.49	162.40	4.02
		1026	159.31	159.95	157.52	
3	4-FBA	527	143.26	143.70	139.82	3.80
		1054	130.86	124.96	121.90	
4	2,3-DFBA	442	155.57	152.17	150.65	4.06
		884	148.07	143.92	138.98	
5	2,4-DFBA	446	140.33	137.72	136.41	4.14
		892	139.93	141.74	140.01	
6	2,5-DFBA	468	159.60	155.07	154.85	3.56
		936	147.40	139.39	134.88	
7	2,6-DFBA	328	111.56	119.11	100.08	4.12
		656	100.77	101.08	104.90	
8	3,4-DFBA	382	127.24	132.59	125.11	3.32
		764	124.69	119.67	128.32	
9	3,5-DFBA	490	151.10	156.01	151.01	4.80
		980	132.85	120.83	125.99	
10	2,3,4-TFBA	465	131.03	116.36	127.75	6.00
		930	136.16	124.43	140.76	
11	2,3,5-TFBA	345	122.58	128.82	131.75	4.20
		690	103.34	106.35	112.00	
12	2,3,6-TFBA	554	116.66	120.31	120.93	6.10
		1108	108.21	109.49	112.05	
13	2,4,5-TFBA	473	128.05	131.03	128.29	4.32
		946	138.05	131.64	133.24	
14	2,4,6-TFBA	242	104.72	109.89	112.12	5.40
		484	105.61	103.56	103.36	
15	3,4,5-TFBA	554	163.98	160.39	162.87	5.96
		1108	151.11	149.42	156.77	
16	2,3,4,5-TetraFBA	304	145.74	161.14	161.98	8.22
		608	156.62	159.99	156.62	
17	2,3,5,6-TetraFBA	298	122.99	118.52	130.29	8.32
		596	131.25	133.00	137.06	
18	2,3,4,5,6-PFBA	350	153.34	148.43	142.68	6.36
		700	139.82	133.49	131.31	
19	2,6-BISFBA	414	NA	NA	NA	6.18
		828	NA	NA	NA	
20	3,5-BISFBA	346	156.21	151.56	162.57	6.24
		692	142.12	140.18	135.85	
21	2-TFM	163	140.82	140.75	141.02	2.60
		326	153.02	148.46	151.55	
22	3-TFM	165	169.86	165.76	161.04	2.68
		330	150.98	148.18	143.38	
23	4-TFM	290	150.37	151.79	156.25	2.62
		480	153.79	147.22	140.02	

[a] Average values are mentioned.

where C_t = concentration of acid at any time t, C_0 = initial concentration of acid.

The curve between ln C_t and time was plotted and fitted to the model, from which the value of K and ln C_0 was determined, considering this reaction as a pseudo-first-order reaction.

The kinetics data were fitted into the straight-line using eqn (v) as the model. The analysis considered the esterification reaction a pseudo-first-order reaction, providing good correlation results. The fitting provided the rate constant (K) value of 1.27×10^{-4} min^{-1} with an R^2 value of 0.95. The fitted curve is represented in Fig. 5.

3.2.4. Reaction mechanism. On the basis of this bifunctionality of MOF, the mechanism given in Fig. 6 can be designed similarly to Fuchineco *et al.*[13] for the esterification of open-chain acid:

The first step involved in the reaction is the hydrogen bonding induced adduct formation of the UiO-66-NH_2 amino group with methanol and the interaction of FBAs oxygen with Zr. The interaction of Zr and O increases the nucleophilic character of the oxygen atom. Along with this phenomenon, the fluorine atom pushes the electron density from the carbon of

 © 2023 The Author(s). Published by the Royal Society of Chemistry

Open Access Article. Published on 02 June 2023. Downloaded on 5/17/2026 5:32:05 AM.
This article is licensed under a Creative Commons Attribution-NonCommercial 3.0 Unported Licence.

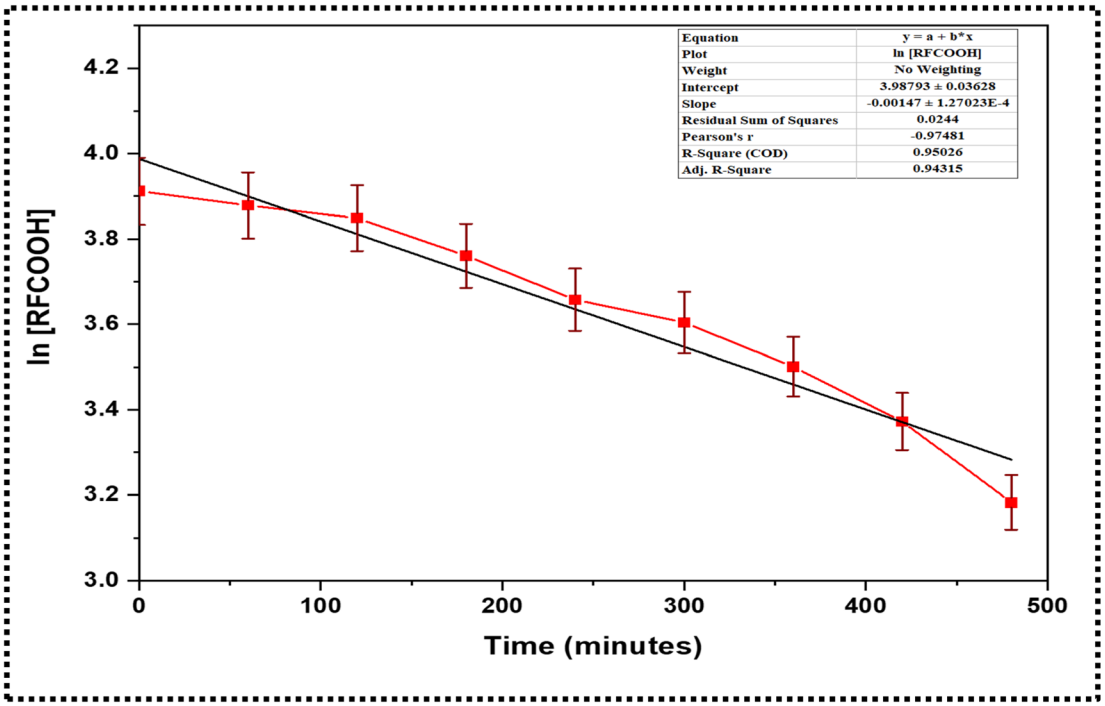

Fig. 5 Kinetic curve of FBAs concentration *vs.* time.

the carboxylic group, due to which the interaction between methanol, oxygen, and this carbon becomes more feasible. Another facilitating factor for this C–O interaction is the hydrogen bonding between the amino group and methanol, which also increases the nucleophilic character of the oxygen. In the last step, the methyl ester of FBAs is formed as the final

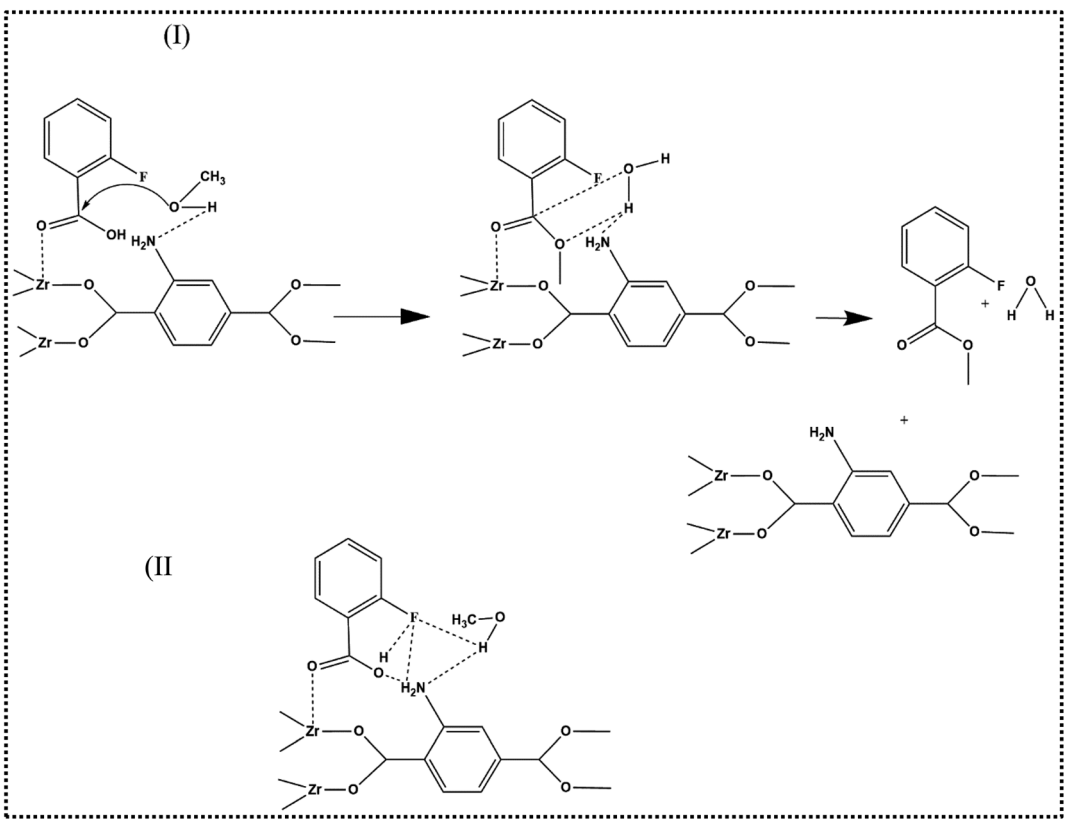

Fig. 6 (I) Esterification mechanism for conversion of 2-FBA to FBAME, (II) other possible hydrogen bonding interactions.

Open Access Article. Published on 02 June 2023. Downloaded on 5/17/2026 5:32:05 AM. This article is licensed under a Creative Commons Attribution-NonCommercial 3.0 Unported Licence.

product, and water as a side product, as shown in Fig. 6(I). However, the intramolecular hydrogen bonding between COOH of FBAs and F may hinder the reaction but depends upon the substitution position of the fluorine atom. Theoretically, other hydrogen bonding interactions can also take place, as shown in Fig. 6(II), so these interactions can be considered as the delaying factor as well as interaction enhancement factor for this reaction.

3.3. Efficiency of UiO-66-NH_2

3.3.1. Esterification of other FBAs with MeOH. The conversion yield was found to be up to 169.86% of the conversion achieved using $BF_3 \cdot MeOH$. Since the conversion yield can also affect the LOD value, this derivatization method was found very useful in achieving the FBAs detection at a very low concentration level. The LOD values were determined using S/N ratio of the peaks, acquired using the software of GC-MS. The LOD determination was done using three replicates of injection and the average value of these three were finalized as the LOD with S/N ratio greater than 3.0. The different LOD values for different FBAs are mentioned in Table 4.

3.3.2. Stability of UiO-66-NH_2. The MOF was separated from the reaction mixture and collected. Thereafter, it was washed two times with water and methanol. Then the solid was dried at 100 °C for 3 hours and used again for the methyl esterification reaction. This activity was repeated for 5 cycles, and no change in the XRD pattern of the MOF was observed, as depicted in Fig. 2(b-ii).

In order to get the impact of reusability on the conversion yield, the reaction was performed up to five repeat cycles and the response of 2-FBA methyl ester was recorded by the GC-MS. As a result, there was no significant change in the activity of UiO-66-NH_2 or in the conversion yield was observed. The results of the GC-MS are provided in Table S4.†

3.3.3. Side products of the reaction. Although the reaction is specific with respect to the esterification and offers a very high yield, many side products are observed as a result of this reaction (listed in Table S3†), but these side products did not interfere with the retention time of FBAMEs. To identify these side products, one sample containing a mixture of three tri-FBAs (2,3,4 + 3,4,5 + 2,4,5) was run in the GC-MS full scan mode (m/z = 50–650) and searched in the MS NIST library. 1,1,3 trimethoxy propane as the first side product was observed, possibly due to condensation of methanol molecules. Similarly, the benzene (1-methoxy 1-methyl ethyl) is also observed. Some of the other esters, like 2,3,4, tri-FBA methyl phenyl ester, and 2,3,4 tri-FBA difluoro phenyl ester, were also observed with the confirmation probability of 9.10% and 6.70%, respectively.

4. Conclusion

Taguchi method offered very reliable results in optimizing the catalytic conversion procedure of FBAs to their methyl esters. The value of R^2 was found to be 0.96, which indicated a good fit for the model. The effects of various parameters were investigated over the defined range, and a regression equation was developed, which can be used to predict the response of the methyl esters at the given conditions. The conversion yield of the pseudo-first-order esterification reaction was calculated with respect to $BF_3 \cdot MeOH$ and UiO-66-NH_2 as a catalyst offered a higher conversion (up to 69.86% more). This drastic change in the conversion reduced the LOD value of FBAs up to trace level, which is a crucial parameter in terms of tracer's analysis. The catalytic procedure described in this study can overcome the disadvantage of a non-recyclable catalyst and longer reaction time in the methyl esterification of FBAs. Therefore, the study simultaneously offers many advantages in terms of FBA analysis; hence the procedure can be followed on a routine basis while analyzing FBAs as chemical tracers.

Conflicts of interest

There are no conflicts to declare.

Acknowledgements

The author acknowledges the Ministry of Education, Government of India, for providing the prestigious Prime Minister Research Fellowship and IIT Roorkee for providing various facilities.

References

1 A. Kumar and C. Sharma, *J. Sep. Sci.*, 2022, **45**, 78–93.
2 K. Müller and A. Seubert, *J. Chromatogr. A.*, 2012, **1260**, 9–15.
3 C. U. Galdiga and T. Greibrokk, *J. Chromatogr. A*, 1998, **793**, 297–306.
4 C. U. Galdiga and T. Greibrokk, *Fresenius. J. Anal. Chem.*, 1998, **361**, 797–802.
5 A. Kumar and C. Sharma, *J. Chromatogr. A*, 2022, **1685**, 463625.
6 S. G. Chopade, K. S. Kulkarni, A. D. Kulkarni and N. S. Topare, *Acta Chim. Pharm. Indica*, 2012, 8–14.
7 I. Riaz, I. Shafiq, F. Jamil, A. H. Al-Muhtaseb, P. Akhter, S. Shafique, Y. K. Park and M. Hussain, *Catal. Rev.: Sci. Eng.*, 2022, 1–53.
8 X. Ma, F. Liu, Y. Helian, C. Li, Z. Wu, H. Li, H. Chu, Y. Wang, Y. Wang, W. Lu, M. Guo, M. Yu and S. Zhou, *Energy Convers. Manage.*, 2021, **229**, 113760.
9 J. M. Marchetti and A. F. Errazu, *Fuel*, 2008, **87**, 3477–3480.
10 A. F. Lee, J. A. Bennett, J. C. Manayil and K. Wilson, *Chem. Soc. Rev.*, 2014, **43**, 7887–7916.
11 M. R. Altiokka and E. Ödeş, *Appl. Catal., A*, 2009, **362**, 115–120.
12 C. Caratelli, J. Hajek, F. G. Cirujano, M. Waroquier, F. X. Llabrés i Xamena and V. Van Speybroeck, *J. Catal.*, 2017, **352**, 401–414.
13 D. A. B. Fuchineco, C. Heredia, S. M. Mendoza, E. Rodr and M. E. Crivello, *Appl. Nano*, 2021, **2**, 344–358.
14 F. G. Cirujano, A. Corma and F. X. Llabrés I Xamena, *Catal. Today*, 2015, **257**, 213–220.
15 R. Sathish Kumar, K. Sureshkumar and R. Velraj, *Fuel*, 2015, **140**, 90–96.

© 2023 The Author(s). Published by the Royal Society of Chemistry

Open Access Article. Published on 02 June 2023. Downloaded on 5/17/2026 5:32:05 AM.
This article is licensed under a Creative Commons Attribution-NonCommercial 3.0 Unported Licence.

16 A. Adnani, M. Basri, E. A. Malek, A. B. Salleh, M. B. Abdul Rahman, N. Chaibakhsh and R. N. Z. R. A. Rahman, *Ind. Crops Prod.*, 2010, **31**, 350–356.
17 Y. H. Tan, M. O. Abdullah, C. Nolasco-Hipolito and N. S. Ahmad Zauzi, *Renewable Energy*, 2017, **114**, 437–447.
18 P. Adewale, L. N. Vithanage and L. Christopher, *Energy Convers. Manage.*, 2017, **154**, 81–91.
19 B. Karmakar, B. Ghosh, S. Samanta and G. Halder, *Sustain. Energy Technol. Assessments*, 2020, **37**, 100568.
20 O. A. Falowo and E. Betiku, *Fuel*, 2022, **312**, 122999.
21 R. Alfredo Quevedo-Amador, H. Elizabeth Reynel-Avila, D. Ileana Mendoza-Castillo, M. Badawi and A. Bonilla-Petriciolet, *Fuel*, 2022, **312**, 122731.
22 N. Sajjad, R. Orfali, S. Perveen, S. Rehman, A. Sultan, T. Akhtar, A. Nazir, G. Muhammad, T. Mehmood, S. Ghaffar, A. Al-Taweel, M. I. Jilani and M. Iqbal, *Molecules*, 2022, **27**, 1–15.
23 S. G. Hosseini, H. Sharifnezhad, Z. Shirazi and N. Zohari, *J. Energ. Mater.*, 2022, 1–19.
24 R. Singh, B. S. Dien and V. Singh, *J. Am. Oil Chem. Soc.*, 2022, **99**, 781–790.
25 P. Kumar, M. Aslam, N. Singh, S. Mittal, A. Bansal, M. K. Jha and A. K. Sarma, *RSC Adv.*, 2015, **5**, 9946–9954.
26 L. Xia, L. Liu, X. Xu, F. Zhu, X. Wang, K. Zhang, X. Yang and J. You, *New J. Chem.*, 2017, **41**, 2241–2248.
27 C. L. Luu, T. T. Van Nguyen, T. Nguyen and T. C. Hoang, *Adv. Nat. Sci.: Nanosci. Nanotechnol.*, 2015, **6**, 025004.
28 M. R. Rezaei Kahkha, A. R. Oveisi, M. Kaykhaii and B. Rezaei Kahkha, *Chem. Cent. J.*, 2018, **12**, 1–13.
29 S. Wu, Y. Ge, Y. Wang, X. Chen, F. Li, H. Xuan and X. Li, *Environ. Technol.*, 2018, **39**, 1937–1948.
30 K. Y. A. Lin, S. Y. Chen and A. P. Jochems, *Mater. Chem. Phys.*, 2015, **160**, 168–176.

© 2023 The Author(s). Published by the Royal Society of Chemistry